Supplementary information for

Enhanced up-conversion luminescence from Er^{3+}, Yb^{3+} codoped $MgAl_2O_4$ nanocrystals through Cr^{3+} incorporation

Savita[1], Madan Murari Upadhyay[2,3], Deepali Jagga[4], Priyanka Bishnoi[5], Kaushal Kumar[6], Ankush Vij[4 *] and Anup Thakur[7, *]

[1]Department of Physics, Chandigarh University, Mohali-140 413, Punjab, India

[2]Optical Materials & Bio-imaging Research Laboratory, Department of Physics, Indian Institute of Technology (Indian School of Mines), Dhanbad-826 004, India.

[3]Noida Institute of Engineering and Technology, Knowledge Park II, Greater Noida-201 310, Uttar Pradesh, India

[4]School of Basic and Applied Sciences, Nirwan University, Jaipur-303 305, Rajasthan, India

[5]Doon University, Dehradun-248 008, Uttarakhand, India

[6]Department of Physics and Astrophysics, Central University of Haryana, Mahendergarh-123 031, India

[7]Advanced Materials Research Lab, Department of Physics, Punjabi University, Patiala-147 002, Punjab, India

E-mail: * vij_anx@yahoo.com
E-mail: * dranupthakur@gmail.com

Figure S1(a) depicts the Williamson-Hall plots for $Mg_{0.94}Er_{0.01}Yb_{0.05}Al_2O_4$, $Mg_{0.9}Er_{0.05}Yb_{0.05}Al_2O_4$, $Mg_{0.89}Er_{0.01}Yb_{0.1}Al_2O_4$ and $Mg_{0.93}Er_{0.01}Yb_{0.05}Cr_{0.01}Al_2O_4$ (tagged as EY1, EY2, EY3 and EYC, respectively) nanocrystals. Figure S1(b) shows the slight negative shift in the diffraction peak corresponding to (311) plane of EY3 sample as compared to other samples.

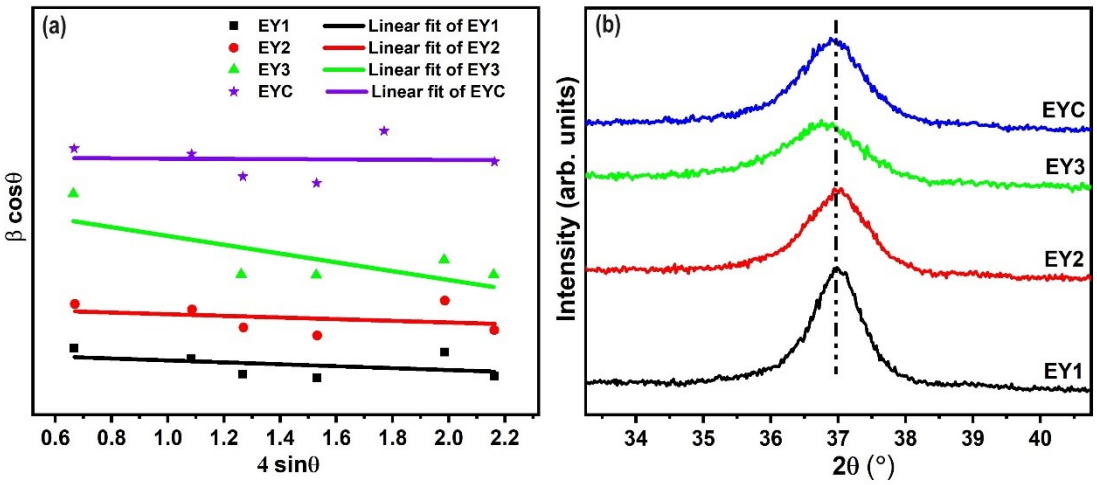

FIG. S1. (a) Williamson-Hall plots and (b) X-ray diffraction peak shift corresponding to (311) diffraction plane of $Mg_{0.94}Er_{0.01}Yb_{0.05}Al_2O_4$, $Mg_{0.9}Er_{0.05}Yb_{0.05}Al_2O_4$, $Mg_{0.89}Er_{0.01}Yb_{0.1}Al_2O_4$ and $Mg_{0.93}Er_{0.01}Yb_{0.05}Cr_{0.01}Al_2O_4$ nanocrystals.

Figure S2 shows the Red to green UC emission intensity ratio (I_R/I_G) at varying pump power for EY3 and EYC samples.

Figure S3 presents the decay curves of $Mg_{0.93}Er_{0.01}Yb_{0.05}Cr_{0.01}Al_2O_4$ and $Mg_{0.99}Cr_{0.01}Al_2O_4$ (tagged as T3a) samples for the 688 nm emission upon excitation at (a) 526 nm and (b) 551 nm, respectively. The lifetimes estimated by single-exponential fitting are 7.56 ns for EYC and 7.25 ns for T3a under 526 nm excitation, and 7.50 ns for EYC and 6.79 ns for T3a under 551 nm

excitation. The slightly enhanced lifetime of Cr^{3+} ions in the codoped sample rules out the possibility of back energy transfer from Cr^{3+} to Er^{3+} or Yb^{3+} ions.

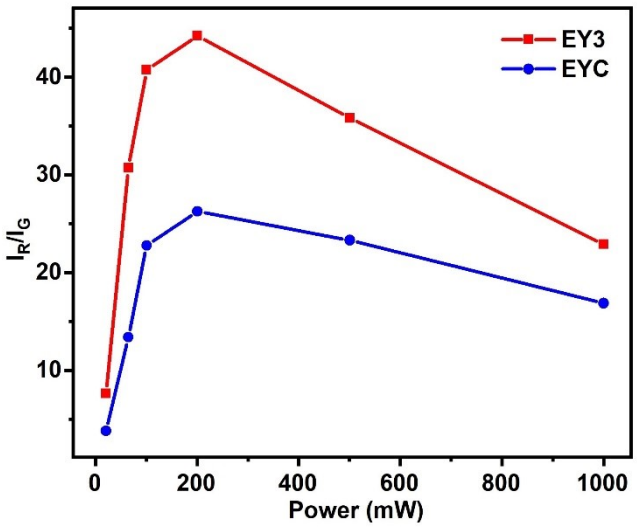

FIG. S2. Red to green UC emission intensity ratio at varying pump power for $Mg_{0.89}Er_{0.01}Yb_{0.1}Al_2O_4$ and $Mg_{0.93}Er_{0.01}Yb_{0.05}Cr_{0.01}Al_2O_4$ nanocrystals.

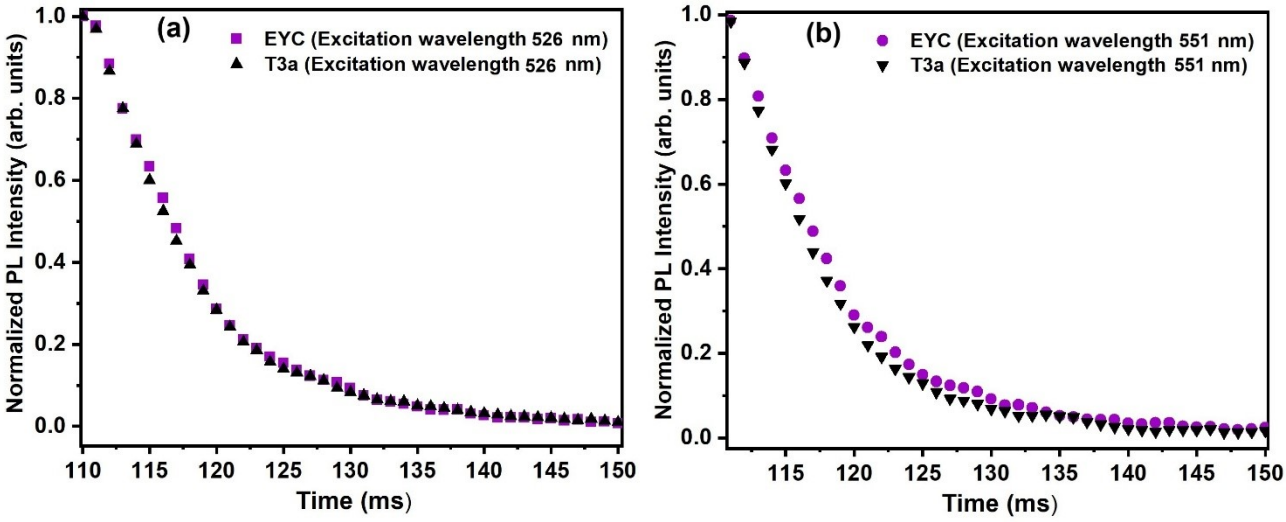

Figure S3. Decay curves of $Mg_{0.93}Er_{0.01}Yb_{0.05}Cr_{0.01}Al_2O_4$ and $Mg_{0.99}\,Cr_{0.01}Al_2O_4$ samples upon excitation at (a) 526 nm and (b) 551 nm wavelengths.

Figure S4(a-c) presents the down-conversion photoluminescence (PL) spectra for EY1, EY2, EY3 and EYC samples at 280 nm, 310 nm, and 405 nm excitation wavelengths. The PL spectra upon 280 nm and 320 nm excitations show broad emission bands ranging in 370-550 nm (blue-violet) and 600-840 nm (red-NIR), characteristic of $MgAl_2O_4$ host. The blue-violet emission band strongly peaked around 400, 420, and 440 nm, with a weak green emission around 532 nm. This blue-violet emission is ascribed to the transitions originating from shallow electron trapping defect centers (F^+, F, and $F^{+2)}$ to shallow hole trapping defect centers (V_{Mg}'' and Mg_{Al}') or to valance band. The very weak emission around 532 nm (indicated by a green colored contour) is ascribed

to $^2H_{11/2} \rightarrow {}^4I_{15/2}$ transitions of the Er^{3+} ions. Furthermore, the red emission around 650 nm may be ascribed to transitions from deep ($V_O^{\bullet\bullet}$, $V_O^{\bullet}$, and V_O^X) to shallow defect states (V_{Mg}'' and Mg_{Al}'), while NIR emission around 715 nm is ascribed to transitions from shallow to deep or between two deep oxygen vacancy states, as discussed in previous research *[Savita, M. Jain, Manju, A. Kumar Sinha, F. Singh, A. Vij and A. Thakur, J. Appl. Phys., 2021, 129, 125111]*.

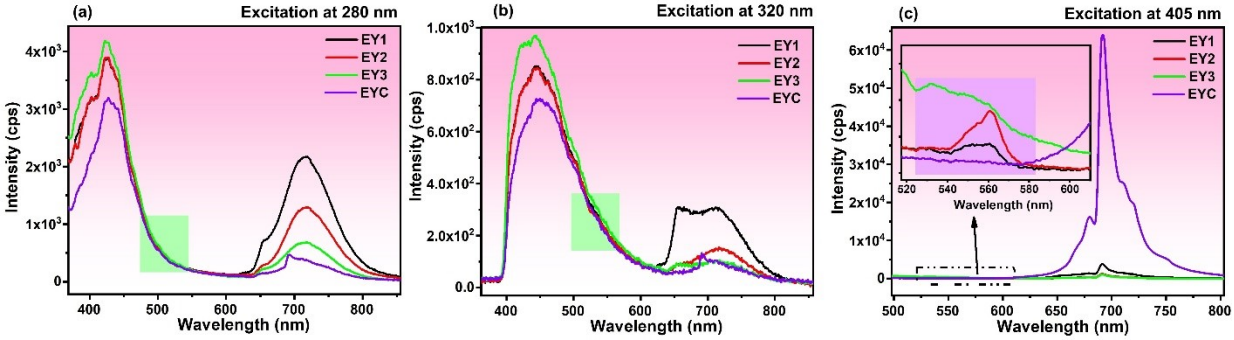

Figure S4. Down-conversion photoluminescence spectra of $Mg_{0.94}Er_{0.01}Yb_{0.05}Al_2O_4$, $Mg_{0.9}Er_{0.05}Yb_{0.05}Al_2O_4$, $Mg_{0.89}Er_{0.01}Yb_{0.1}Al_2O_4$ and $Mg_{0.93}Er_{0.01}Yb_{0.05}Cr_{0.01}Al_2O_4$ nanocrystals upon excitation at (a) 280 nm, (b) 320 nm, and 405 nm wavelengths.

Moreover, the EYC samples shows deep red emission around 688 nm, attributed to *d-d* transitions of the Cr^{3+} ions along with its Stokes and antistokes sites bands *[Savita, P. Vashishtha, G. Gupta, A. Vij and A. Thakur, J. Phys.: Condens. Matter, 2023, 35, 115303]*. This Cr^{3+} dopant assisted emission upon UV excitation reveals the energy transfer between intrinsic defects and Cr^{3+} ions. The decreased host defect assisted emission in the EYC sample, possibly due to an increase in the energy transfer from defects to doped (Er^{3+}, Yb^{3+}, and Cr^{3+}) ions.

Further, PL emission upon 405 nm excitation shows the Er^{3+} ion assisted emission in 520-570 nm range (shown in inset) and Cr^{3+} ion assisted emission in 650-760 nm range. It has been observed that Er^{3+} ion assisted emission is quenched in EYC sample, while Cr^{3+} ion assisted emission is enhanced, that anticipate the energy transfer between Er^{3+} and Cr^{3+} ions through defect centers.